

# SUTED4L - STUDY FOR THE APPLICATION OF THE FLYEYE TELESCOPE TO THE SURVEY OF THE HIGH-LEO ORBITAL REGION

Roberta Pellegrini<sup>(1)</sup>, Piero Gregori<sup>(1)</sup>, Francesco Cerutti<sup>(1)</sup>, Linda Dimare<sup>(2)</sup>, Fabrizio Bernardi<sup>(2)</sup>, Davide Bracali Cioci<sup>(2)</sup>, Elena Vellutini<sup>(3)</sup>

<sup>(1)</sup> OHB Italia SpA, via Gallarate 150, 20151 Milano (Italia), Email: info@ohb-italia.it

<sup>(2)</sup> SpaceDyS Srl, via Mario Giuntini 63, 56023 Pisa (Italia), Email: info@spacedys.com

<sup>(3)</sup> Agenzia Spaziale Italiana, via del Politecnico snc, 00133 Roma (Italia), Email: urp@asi.it

## ABSTRACT

The observation of LEO region is a challenging task to be executed with optical sensors: the SUTED4L study has the aim to show the efficiency of a network of Flyeye telescopes in carrying out the HLEO region survey. Realistic simulations are performed to address all the driving difficulties of the task: the Network architecture was defined considering the number and the location of observational sites and the number of sensors present at each observatory. An observation strategy is also defined and implemented in the simulation, tailored on the orbital characteristics of the target objects (HLEO) and on the sensors (Fly-Eye architecture). Based on a Flyeye Telescope model, derived from actual instrument development outcomes, the simulations allowed to assess the detection performances in a realistic scenario. This work presents the overall SUTED4L study, including the simulations and the analyses performed.

## 1 INTRODUCTION

The safety and security of economies, societies and people rely on space-based applications such as communication, satellite navigation and meteorology. Today, space debris is one of the principal threats to satellites: an accurate and complete catalogue of space objects is therefore needed to mitigate the risk of in orbit collisions. Space surveillance activity refers to the ability to detect, catalog and predict the trajectories of space objects orbiting the Earth. In this complex scenario, the sensors are the key assets allowing to observe the sky and discover space objects, both natural (asteroids) and manmade (satellites and debris). The Flyeye telescope, with its unique features (the extremely large Field-of-View coexisting with seeing-comparable pixel size and precise and fast positioning capabilities), can play a key role in discover and reobserve space objects, and is based on an innovative optical design conceived by OHB-I nearing completion. In particular, the Flyeye telescope can be tailored to carry out optical surveys of the space debris population with an unprecedented efficiency. This makes it an important asset both at national level and within the

Space Surveillance programs of the European Union, such as the EUSST initiative and its future evolution. Four Fly Eye telescopes have been financed in September 2022 by the Italian Space Agency: this first Fly Eye Network will be the new space sentinels based on OHB-I technology that will survey the sky in search of space debris.

Former studies (e.g. SUTED – Study for the application of the Flyeye Telescope to the survey of the MEO orbital region) have shown that a network of worldwide distributed Flyeye sensors allow to successfully implement surveys in MEO and GEO orbital regimes. The observation of LEO region, performed so far by radar assets, is a challenging task to be executed with optical sensors: the SUTED4L study, performed in the frame of an ASI contract, has the aim to show the efficiency of a network of Flyeye telescopes in carrying out the HLEO region survey. In the frame of this study, the features of the Flyeye telescope are exploited and coupled with advanced image processing algorithms, suitable for tracklet detection, and efficient orbit determination SW. Realistic simulations are performed to address all the driving difficulties of the task, so that the final results are reliable to evaluate the efficiency of the system. The Network architecture was defined considering the number and the location of observational sites and the number of sensors present at each observatory. An observation strategy is also defined and implemented in the simulation, tailored on the orbital characteristics of the target objects (HLEO) and on the sensors (Fly-Eye architecture).

Based on a Flyeye Telescope model, derived from actual instrument development outcomes, the simulations allowed to assess the detection performances in a realistic scenario (illumination, weather conditions, Earth shadow, debris dimensions, etc.). This model allows to simulate the generation of optical observations, using a commercial propagator integrated with specifically developed SW modules. The observations were subsequently processed for performing orbit determination and catalogue build up, allowing a comparison with the initial target population (the ‘ground truth’), to obtain a detailed analysis of the expected

optical network performances. This work presents the overall study, the simulations and the analyses performed up to now during SUTED4L study.

## 2 STUDY FLOW, ASSUMPTIONS AND CONSTRAINTS

The SUTED4L study has the main aim to assess the performances of a network of Flyeye telescopes for the observation and cataloguing of High LEO objects (HLEO), orbiting between 1000 and 2000 km altitude. In order to validate the proposed system, realistic simulations have been performed: the term “realistic” means that all the driving difficulties of the task are addressed, so that the obtained results are reliably significant in terms of object population coverage, catalogue build up and catalogue maintenance.

The main assumption is the construction of a catalogue of orbits from scratch, using exclusively the observations obtained from the considered network of Flyeye sensors, operating in survey mode, therefore with no a-priori knowledge of the objects to be observed. The maintainability of the constructed catalogue is simulated as well, using only survey observations from the same network.

These are extremely conservative hypotheses. The results obtained should then give an estimation of the minimum obtainable performances.

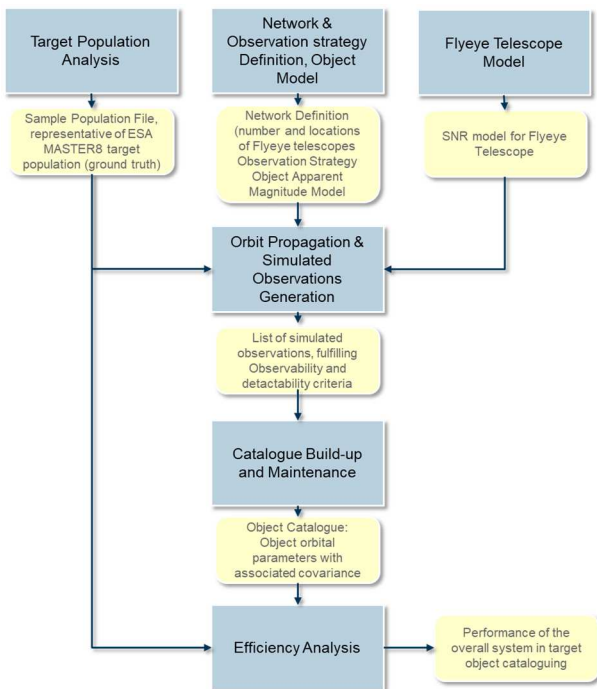


Figure 1: Simulation Flow

In Fig. 1, the simulation flow is depicted. The adopted population, used as ground-truth, has been extracted from

the ESA MASTER8 population, and is a statistically significant sample of the HLEO target population, representative of the original population in terms of orbital characteristics and object sizes. The simulation cycle starts from the generation of the simulated optical measurements, passes through the data processing and ends with the catalogue of orbits.

The output of such simulations obviously depends on all the imposed assumptions, (e.g., target objects characteristics, observation site selection and network architecture, telescope characteristics, observation strategy, physical observation conditions, meteorological constraints, etc.).

Such assumptions are briefly described in the following.

### 2.1 HLEO Population Sample

In the SUTED4L study, the selected full population sample contains 999 objects, randomly extracted from the reference MASTER-8 population, including:

- 22% of HLEO objects with diameter greater or equal to 10 cm, for a total of 874 objects;
- 1% of LEO objects transiting under and above 1000 km altitude (LLET), with diameter greater or equal to 10 cm, for a total of 49 objects;
- 1% of objects transiting in LEO and higher regions (LEOT), with diameter greater or equal to 10 cm, for a total of 76 objects.

Some preliminary analyses have been also performed using a subset of this population, composed of 99 objects randomly extracted from the reference population.

### 2.2 Network Selection and Observation Strategy

The observation strategy, in order to be effective, should be tailored on the target population we want to consider. For example, NEO, GEO, MEO and HLEO targets have typically different observing strategies, due to their different sky proper motion and observability constraints.

During the SUTED4L study two different approaches have been considered:

- *Equatorial fence*, consisting in a strategy that covers the regions along the equator with the purpose that all the considered debris that will cross this region will be observed for sure.
- *Phase-aware fence*, consisting in a strategy that focuses on detecting debris at their most favourable phase angle (the angle observer-target-Sun).

Both of these strategies have to take into account the projection of the Earth shadow onto the Sky Plane and the effect of the object phase angle. Concerning HLEOs, we have to consider that the targets are orbiting very

close to ground, and this implies that the sky proper motion is very high (several hundreds of arcseconds per second) and that the Earth shadow at their typical altitude (1000-2000 km) is dominating; the observability window is limited to the time just after sunset and before sunrise. During the middle of the night the HLEOs are always in shadow and therefore are not observable by passive sensors such as optical telescopes. This geometrical consideration translates into around two hours of observing time (it actually depends on the location latitude and season) after sunset and two hours before sunrise.

The finally selected strategy is a mixed approach, observing the border of the Earth shadow @1000km of altitude, where the debris is brighter (since its phase angle is the minimum possible just outside the shadow), and adding a portion of equatorial fence, near to the Earth shadow cone. The portion of equatorial fence has been added to improve the observability of certain classes of objects, such as a sun-synchronous orbit objects, that are rarely observed with a pure phase aware strategy.

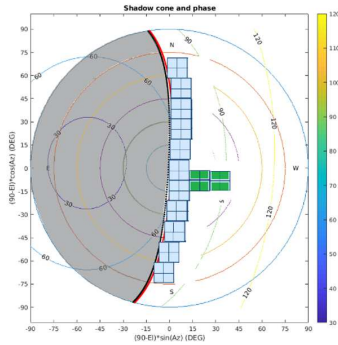


Figure 2: Example of mixed strategy implementation. Gray: Earth Shadow cone (in red its border). Light Blue: Phase aware fence. Green: equatorial fence portion

The image exposure time for HLEO application is assumed to be 1s, in order to limit the trailing loss effect (avoiding too long trails: very fast objects in HLEO belt can have angular speed up to 1500arcsec/s, thus 1000 pixel/s).

Concerning the Network definition, i.e. the number and location of Flyeye telescopes, the driving criteria are:

- the possibility to observe the object at each favourable pass over the observing station (due to the high angular speed of HLEO objects, 3 telescopes for each station have been considered)
- the necessity to deal with the meteorological factor and to have enough stations longitudinally distributed to have the possibility to observe the target objects with the required frequency.

Such considerations lead to the choice of a “full network” composed of seven stations, each equipped with three Flyeye telescopes. The definition of the observing sites depends by several issues, some related to the site performance, others related to geographical distribution and local service availability.

The site performance basically depends upon these parameters:

- Number of clear nights in a year;
- Average seeing;
- Sky darkness;
- Winds;
- Low humidity.

The geographical distribution is important to guarantee the proper sky coverage on both Earth hemispheres, and to avoid seasonal effects (e.g., summer time has shorter nights). It is also important that the sites are far enough from each other to minimize the meteorological correlation: if two sites are too close, it is very likely that if it is cloudy in one site, it is cloudy in the other site as well.

The proposed site selection is included in Tab. 1.

Table 1: Full Network sites selection

| Station    | Latitude [deg] | Longitude [deg] |
|------------|----------------|-----------------|
| Matera     | 40.649169      | 16.704207       |
| New Norcia | -31.048333     | 116.191944      |
| Tucson     | 31.958333      | -111.596667     |
| La Silla   | -29.261167     | -70.731333      |
| Haleakala  | -20.7083       | -156.2571       |
| Teide      | 28.300917      | -16.511806      |
| Malargue   | -35.773333     | -69.399722      |

### 2.3 Flyeye Telescope Features

The sensors (telescopes) are the key assets allowing a successful observation of the sky to discover space objects, both natural (asteroids) and manmade (satellites and debris). The Flyeye telescope represents the core HW technology. It is based on an innovative optical design conceived by OHB-I and a patented technology, named Fly-Eye, which consists in splitting the overall FoV in sub FoVs on which an array of correctors elements is placed, in form of distributed contained size lenses, so making easier the correction of aberrations. This innovative telescope solution allows the implementation of a modular and compact design. This telescope grants high sensitivity and accuracy in an extremely wide Field of View (44 sq. degrees) without gaps, and an astronomic resolution tailored for the Observatory sites (1.5 arcsec).

In Table 2 the key features of the Flyeye Telescope are

summarized.

Table 2: Flyeye Telescope main features

|  |                      |
|--|----------------------|
| Aperture Diameter                                      | one meter class      |
| Entrance Pupil Shape                                   | Circular             |
| Field of View  | 6,7deg x 6,7 deg     |
| Pixel Scale  | 1.5"x1.5"            |
| Pixel Size   | 15 $\mu$ m           |
| Axes maximum speed                                     | 7deg/s               |
| Axes max. acceleration                                 | 12deg/s <sup>2</sup> |
| Repositioning time (adjacent FoV), incl. image readout | 4s                   |

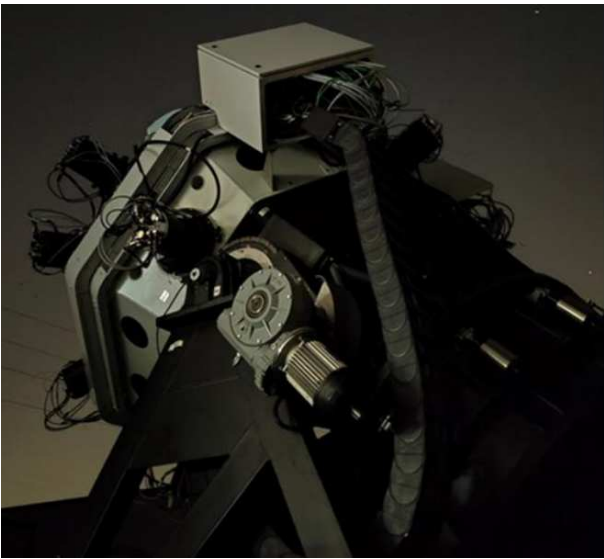


Figure 3: Picture of the Flyeye Telescope prototype

## 2.4 Observations Concepts

Optical observations have the advantage of exploiting the abundant radiation provided for free from the Sun. On the other hand, they have constraints resulting from the physics of the observation process. Because the source of light illuminating the satellite/debris is the Sun, an essential requirement is that the object is outside the shadow cone of the Earth. Moreover, the optical ground sensor cannot operate unless the ground station is inside the same shadow cone. Last but not least, there are meteorological constraints: a simple cloud cover is sufficient to prevent any optical observation.

Once these fundamental observation conditions are satisfied, the possibility to actually detect a particular object depends on the signal to noise ratio (SNR) of the source acquired by the sensor.

All these considerations lead to the identification of two

different concepts, namely the Observability and Detectability conditions.

**Observability:** an object passing over a station is observable at a specific time if the sun light reflected by the target object could be readable by the selected ground station telescope. It is mostly related to geometrical constraints (e.g. elevation angle, sun below horizon, etc.)

**Detectability:** Once the Observability conditions are satisfied, the factors allowing to detect a particular object must be analysed (SNR condition). The possibility to detect the object trail is fundamentally dependent on the object apparent magnitude and angular speed, on the sensitivity of the applied optical sensor, and on the performances of the SW used to detect the trail from the acquired image.

## 2.5 SW performances assumptions

Even if the sensors are the key assets for a successful survey campaign, both the results about the rate of discovery and cataloguing of new space debris and the results about catalogue maintainability strongly depend not only on the Flyeye sensor capabilities, but also on the algorithms used for trail detection, initial orbit determination (IOD) and correlation.

For the trail detection, we assume to exploit an efficient tool for automatic trail detection able to detect very faint trails, namely the ATIP software [1]. ATIP software is able to sum up the signal along the trail, thus detecting faint trails with a low rate of false detections (about 2%). This tool is not directly used in simulations. The simulated trails are filtered on the basis of the minimum detectable SNR, which is derived from ATIP theoretical performances, as obtained from the test campaigns performed so far on synthetic images.

The computation of preliminary orbits is a fundamental step for space debris discovery. Two or more trails can be considered as belonging to the same object, still unknown, only if an orbit is found which fits them all. The software DEBORB, which is used for data processing in the presented study, implements a modern algorithm of the class of Keplerian Integral methods [2,3]. These methods are able to determine a 6-parameter orbit from a couple of trails observed at different passes. This is a big advantage with respect to classical methods, such as Gauss' and Laplace' ones [4], which requires at least 3 observations per pass to compute a preliminary orbit. This allows us to decrease the number of telescopes to be used for each observing site and moreover it implies a reduction of the computational cost for the step of discovery.

Finally, for the correlation of new survey observations to already known orbits, DEBORB implements the multi-filter attribution algorithm described in [5].

All the above cited algorithms contribute to the results

presented in this paper. If even only one of them is substituted with another, the achievement of such results is no more guaranteed.

### 3 ORBIT PROPAGATION AND OBSERVATIONS SIMULATION

The orbit propagation and observation simulation approach is described hereafter.

Each object of the population sample is propagated using an off-the-shelf simulation tool. AGI System Tools Kit (STK) has been selected to be used because it performs complex analysis of space assets and it allows to define relationship between the different objects integrated into a defined scenario.

The STK computation produces as report the list of debris/satellite possible observations during observability periods between the observatory and object: position data in terms of Right Ascension and Declination wrt the selected observatory, time, distance from the observatory, phase angle. All these data are stored in a .txt file made available for the observation simulations generation.

Other functions, e.g. the actual observation extraction and the corresponding SNR calculation, need to be developed in a different environment. The MATLAB environment has been selected since it both offers the necessary mathematical and computational capabilities and is already predisposed to be interfaced with STK. So dedicated MATLAB scripts/functions have been created.

The MATLAB tool processes the STK generated .txt file, filtering and checking the validity of the simulated observation considering the selected observation strategy. The station meteorological conditions are taken into account in a dedicated filter applied just before the Orbit Determination activities. The apparent magnitude and SNR are then computed, and a random error is applied to RA, DEC and magnitude values.

Finally, the list of simulated observations is stored in a file to be used by the Orbit Determination algorithm.

So, in order to generate the simulated optical measurements, the following steps have been followed:

- a. Each object in the population file is propagated for the simulation duration (6 months)
- b. For each station in the network, the object observability periods have been computed
- c. The selected observation strategy (tailored for the HLEO application) is implemented, generating none, one or more observations for each object pass, depending on the fulfillment of all the constraints and on the object residence time within the observed sky fence
- d. For each actual observation, the SNR ratio of the trail is computed. Assuming the availability of

the ATIP advanced trail detection image processing algorithm, a very conservative constraint is adopted: the trail is considered detectable (and therefore used for OD) only if  $SNR_{trail} \geq 6$  on both trail extrema.

- e. Each trail is identified by its extrema (starting and ending pixel in RA-DEC coordinates, with the associated time stamp). The astrometric error is simulated as well, adding a random error to RA-DEC coordinates whose RMS is function of the pixel SNR (the fainter is the trail, the higher is the error RMS).

Some additional assumptions about the observation sites environmental conditions have to be made to calculate the SNR of the trail, namely the values for mean seeing condition and sky background.

The mean seeing is assumed to be 1.2 arcsec, while the mean sky background is set to 19.5. In particular the assumption on sky background is quite conservative and takes into account also for the observation strategy constraints. Indeed for HLEO objects the observation session needs to start as soon as possible to maximize the available time slot, even if the sky is not fully dark (sun 10/12 deg below horizon). The seeing assumption is a realistic mean value, since in the network are included sites with a better seeing condition (typically 0.7-0.8 arcsec for Chilean and Hawaiian sites), but also sites with worse conditions (e.g. Matera site has a typical seeing of 1.5 arcsec).

The adopted SNR model is the actual Flyeye telescope SNR model, considering the telescope HW improvements foreseen in the frame of the ASI contract for the first Flyeye SST network implementation (e.g. a reduction of the central obstruction w.r.t. the first Flyeye prototype) and the measured performances of astronomical cameras in terms of gain, readout noise and dark current.

As anticipated above, the observation generation process also includes meteorological factor (the telescope cannot observe if clouds are present).

For this purpose public-domain data obtained from the NASA ISCCP (International Satellite Cloud Climatology Project) project, part of the NOAA-NCEI department (National Oceanic and Atmospheric Administration, National Centers for Environmental Information) have been used, in particular the mean nocturnal cloud coverage in a 5-year time period has been calculated for each day of the year. A "score index" has been then assigned to each day, to distinguish between clear or cloudy nights. The simulated observations are considered valid only if the observation night is clear.

### 4 ORBIT DETERMINATION AND EFFICIENCY VALIDATION

The observation of a trail appearing in the image resulting from a single exposition is stored in the form of two detections, defining the position of the start and end of the trail. The measurements of the positions on the celestial sphere are given using right ascension and declination in the topocentric equatorial frame, centred at the observer. A couple of detections, defining the beginning and the end of a trail, is a *tracklet*.

Given a set of tracklets, obtained from optical survey observations, it is necessary to establish which of them belong to the same object. The computational cost of the correlation of  $k$  tracklets, given an input set of  $N$  tracklets, without a priori knowledge of the orbits of the observed objects, has order  $N^k$ . Since a Keplerian integral method is used for IOD [2], the very first step is correlating couples of tracklets and this requires  $N^2$  computations, which is the minimum possible cost.

The basic idea of this method is to compute a two-body orbit fitting the two tracklets starting from the conservation of the first integrals of the two-body problem, namely the total energy and the Lenz vector. In addition, a variant of the method can be used, which takes into account the nodal precession due to the quadrupole term of the Earth geopotential. Since we want to correlate tracklets of different passes and also because low altitude objects are among the ones to be catalogued, this effect is not negligible and it must be considered since the first step of preliminary orbit computation. Once a preliminary orbit has been found, differential corrections are performed starting from it, in order to obtain a solution that minimises the residuals. Only if the differential corrections converge to a solution with acceptable residuals, the correlation of two tracklets is accepted.

Correlations involving only two tracklets are likely to be false, which means that they do not correspond to the real objects observed. There are mainly two ways a correlation can be false. One possibility is that it links two tracklets belonging to two distinct objects. Another possibility is that the associated orbit is very far from the real one.

A correlation can be considered reliable only if new tracklets are successfully added to the orbital fit and the observation residuals decrease after the addition of the new tracklets. The procedure implemented to recursively correlate new tracklets to a known orbit and improve the orbital fit is called attribution and is described in [5].

The processing works as follows. The first step consists in finding 2-tracklet correlations through the usage of the Keplerian Integrals method (IOD). Then, the attribution algorithm is applied to any 2-tracklet correlation in order to obtain 3-tracklet correlations. Finally, the last step, called *correlation management*, consists of removing the duplicates and merging (or discarding) correlations.

It is not realistic nor convenient to process together all the observations generated for the entire time interval covered by the simulation. The reason is twofold:

- The computational cost of the IOD (2-tracklet correlations) is  $N^2$ , where  $N$  is the number of tracklets,
- In reality the observations from a single site are obtained and processed day by day.

In the simulations of this study, the simulated observations can be processed as they were obtained day by day. A different split of the set of observations can be applied, if this comes out to be more convenient in terms of simulation runtime. In practice, the entire set of simulated observations is divided in  $M$  subsets, each corresponding to a single day or to any pre-defined interval of time. The  $M$  batches of observations are processed sequentially, following a temporal order. The batches of subsequent time intervals are processed one after the other, so that the results obtained after the processing of the  $n$ -th batch of data are used as input for the processing of the  $(n+1)$ -th batch of data.

The catalogue construction is assumed to be performed from scratch, without any a priori knowledge about the orbits of the observed objects. This means that we do not know which observations belong to which object. The software takes in input the first batch of observations and computes initial orbits fitting couples of tracklets. Then a step of attribution is performed in order to obtain 3-tracklet correlations. After this, only 3-tracklet correlations are retained and submitted to the process of correlation management. The output of this block of operations (Block A) includes the database of normalized correlations and the set of tracklets left uncorrelated.

The output of Block A is passed to a second block of operations (Block B) together with a new batch of observations. The software performs first the recursive attribution of new tracklets to the known orbits, using as input tracklets the left tracklet coming from the Block A and the tracklets of the new batch. The known orbits are the ones given as output by the Block A. The obtained database of correlations is submitted to the correlation management process, so that the output of the block includes the database of normalized correlations and the set of tracklets left uncorrelated.

The tracklets left uncorrelated after Block B operations are given in input to the Block A to find new discoveries. Hence the process is repeated for each new batch of observations, starting with the operations of Block B and then performing the processing of tracklets left uncorrelated with Block A. The iteration scheme is graphically represented in *Figure 1*.



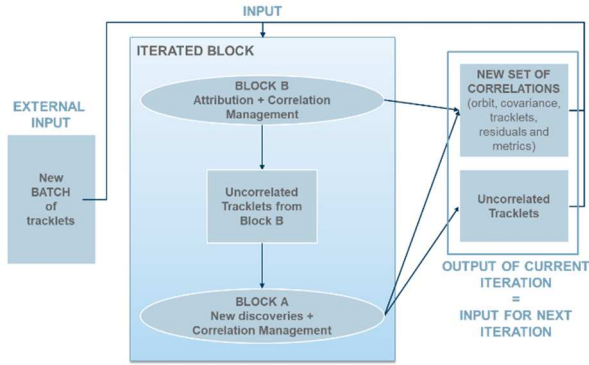


Figure 1: General iteration scheme.

#### 4.1 Cataloguing and numbering criteria

A very important step of the simulation is the decision of when a correlation contained in the provisional catalogue becomes “good enough” to be inserted in the definitive catalogue. In other words, a cataloguing condition has to be defined. It is important to note that the percentage of catalogued objects (and therefore the performances of the system) significantly changes using different cataloguing criteria.

In the lack of a commonly accepted criterion among the European scientific community for the cataloguing of space debris, two possible choices have been considered for this study.

The first one was to consider the observed arc. Only having observations covering a big portion of an orbit we can compute a reliable orbit. Hence, the number of tracklets can be used as a possible basis to judge if a correlation could be inserted in the catalogue.

The second possibility was to consider the orbital formal accuracy computed using the covariance. Only orbits that maintain a good formal accuracy for a certain number of days can be good enough to be used for services like the collision avoidance or the fragmentation analysis.

It has been decided to adopt as definition of “catalogued” object a requirement coming from the ESA studies performed in the frame of the SSA-SST programme (“Space Situational Awareness – Space Surveillance and Tracking System Requirements Document” SSA-SST-RS-RD-0001). Hence, an object is considered as catalogued if its accuracy 48 hours after the end of the simulation is within a fixed envelope defined in the RTW local orbital frame.

The RTW frame is centred in the object and its axes are defined by the radial, transversal and out-of-plane directions. The envelope for LEO objects in the RTW frame is:

$$[40 \text{ m}, 200 \text{ m}, 100 \text{ m}]$$

The above limits apply to the  $1\text{-}\sigma$  error in position in the RTW local frame centred in the object.

## 5 RESULTS

After the completion of all simulation tasks, it is possible to evaluate the performances of the network both in terms of telescope network and related observation strategy efficiency, and in terms of obtained catalogue w.r.t the original population (ground-truth).

The time distribution of the observations of an object is a significant feature to be analysed to evaluate the efficiency of the telescope network and related observation strategy. Indeed, too long and frequent gaps in the observations prevent the possibility to catalogue the object or to maintain an already catalogued one. Therefore, a coverage analysis of the simulation can give preliminary information and prediction of the achievable cataloguing capability.

For each object, the simulated observations, properly filtered to remove too faint trails ( $\text{SNR}_{\text{trail}} < 6$ ) and observations acquired during cloudy nights, are sorted in chronological order, allowing to calculate the revisit time between consecutive observations. The mean, max and standard deviation of such revisit time values are computed to give an indication of the survey efficiency.

Following the catalogue construction, is furthermore possible to calculate the percentage of discovered objects (i.e. 3-tracklet correlations have been found for them, allowing their insertion in the provisional catalogue) and catalogued objects (i.e. objects fulfilling the accuracy envelope cataloguing criteria and therefore inserted in the final catalogue) w.r.t. the ground-truth.

#### 5.1 Results for the reduced population sample

For a preliminary assessment of the performances of the network and of the selected strategy, a reduced population of 99 objects greater than 10 cm was randomly extracted from this sample. This population is summarised in *Table 3*.

Table 3: Reduced population sample used for preliminary simulations in SUTED4L (99 objects).

| HLEO | LLET | LEOT | Total |
|------|------|------|-------|
| 88   | 4    | 7    | 99    |

The coverage analysis figures after 2 months of survey is depicted in the following figures.

From these figures, it can be deduced that worst results belong to small transient objects, and resident objects in polar-orbit (sun-synchronous objects).

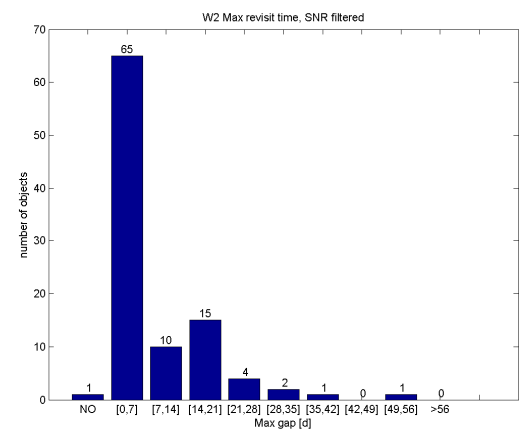
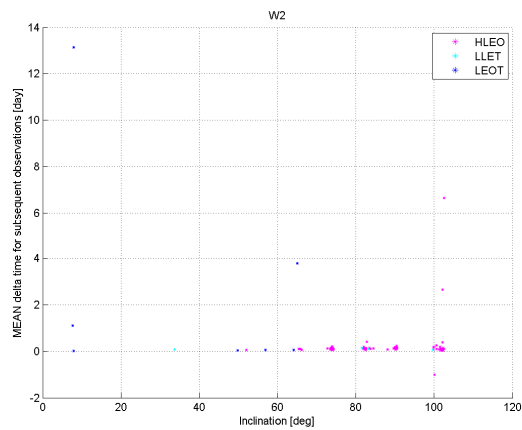
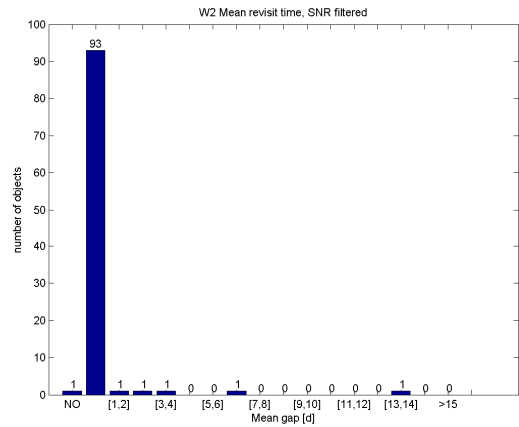
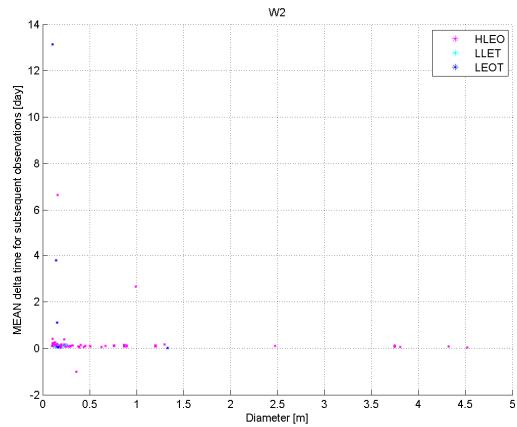


Figure 2: Mean revisit time values as function of size (top) and inclination (bottom). 99 objects, 2 months of survey. Negative values correspond to Not-Observed objects (NO)

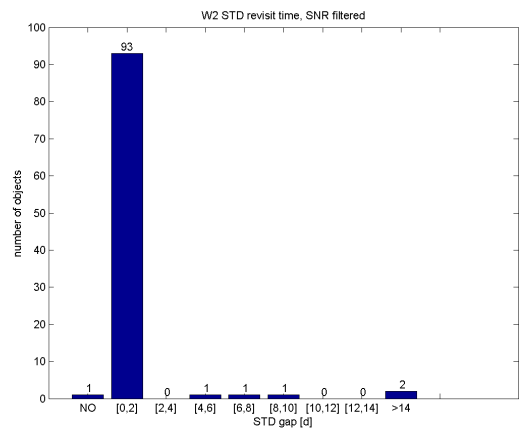
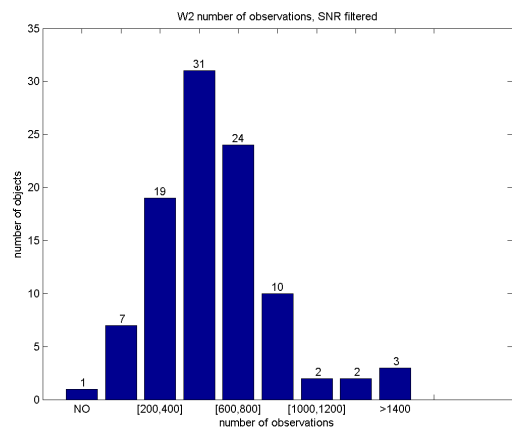


Figure 4: Histograms for mean, max and STD of revisit time values. 99 objects, 2 months of survey

Figure 3: Histogram of number of observations, 99 objects, 2 months of survey.



The results of the catalogue build up and maintenance obtained after 2 months of survey for the reduced population are summarised in Table 4.

Table 4: 99 objects, Cataloguing results after 2 months of simulation.

| Days                       | After 7 days | After 28 days | After 60 days |
|----------------------------|--------------|---------------|---------------|
| Catalogued                 | 64           | 91            | 94            |
| Discovered (without dupl.) | 86 (84)      | 95 (93)       | 99 (95)       |

### 5.2 Preliminary results for full population sample

The simulation for the full population (999 objects) is currently on-going and not yet completed. Preliminary figures are provided here in the following for coverage analysis only.

The statistical distribution of revisit times is quite similar to the one obtained for the 99 objects population, therefore similar results in cataloguing performances are expected as well.

As per the reduced population simulation, also for the full 999 objects population the worst coverage results belong to small transient objects, and resident objects in polar orbit (sun-synchronous objects). In order to improve the cataloguing performances for sun-synchronous objects, the implementation of an ad-hoc observation strategy could be considered.

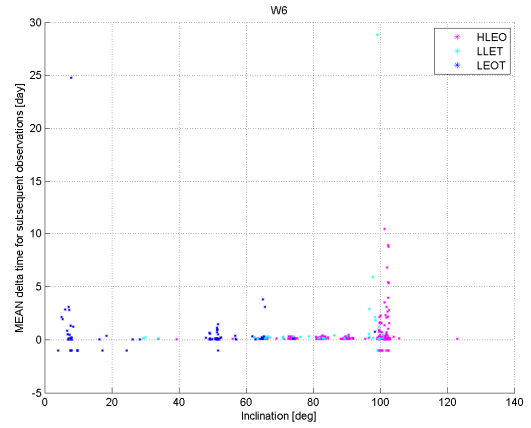


Figure 5: Mean revisit time values as function of size (top) and inclination (bottom). 999 objects, 2 months of survey. Negative values correspond to Not-Observed objects (NO)

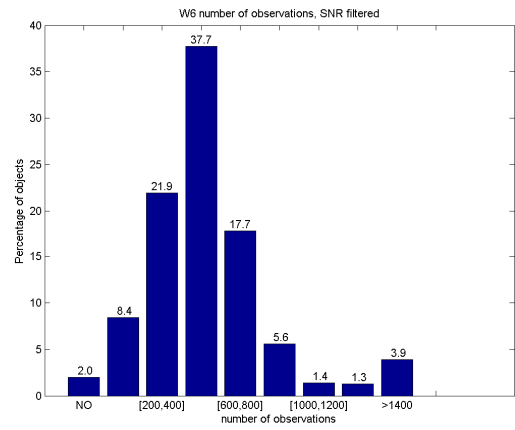
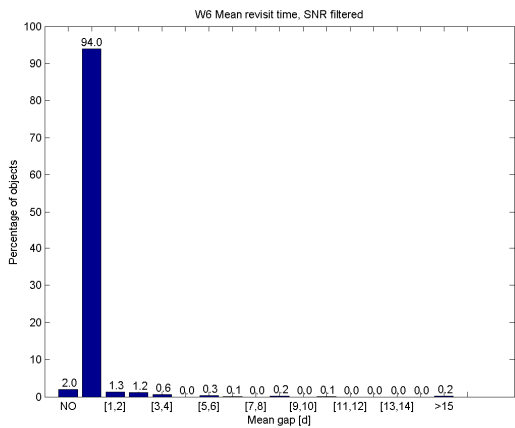
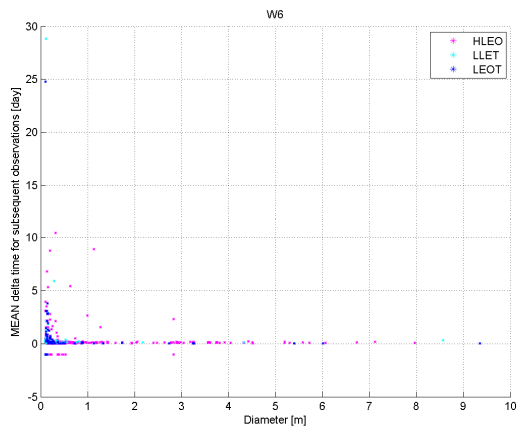


Figure 6: Histogram of number of observations, 999 objects, 2 months of survey.



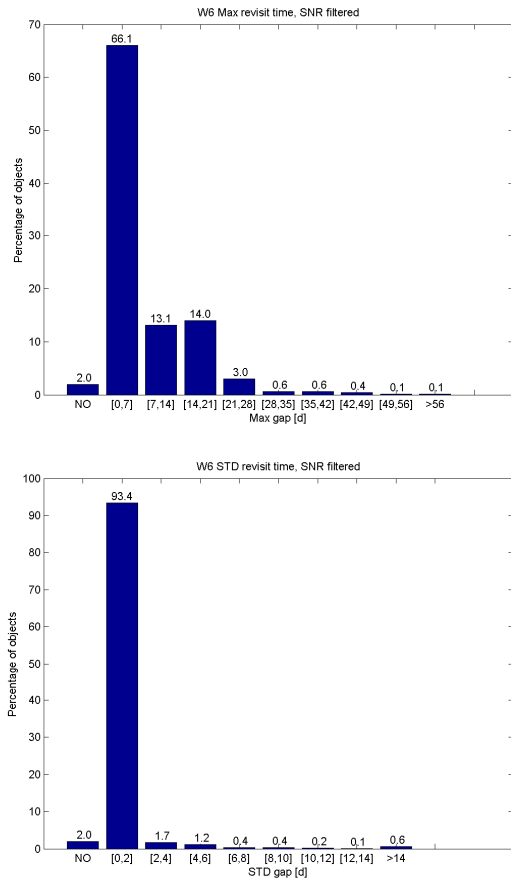


Figure 7: Histograms for mean, max and STD of revisit time values. 999 objects, 2 months of survey

## 6 CONCLUSIONS

Regarding the HLEO SST application a network comprising 7 astronomical stations, properly worldwide distributed, hosting 3 Flyeye telescopes can successfully perform optical survey of the HLEO belt, guaranteeing high performances in cataloguing HLEO objects with a diameter bigger than 10 cm.

The adoption of high performances SW for OD tasks allows to build-up and maintain the catalogue starting

from scratch. The maintenance of catalogue could also take advantage of follow-up observations if needed.

The implementation of the first “baseline” Flyeye network, composed of four Fly Eye telescopes, has been financed in September 2022 by the Italian Space Agency. Even if its primary scope is the survey of MEO and GEO optical belts, such network could be also used for other SST applications such as the HLEO survey. Due to the reduced number of sites and telescopes, its performances in HLEO application cannot reach the ones foreseen in the SUTED4L study for the full network configuration, but it will allow a first on-the-sky test of the Flyeye telescopes, the new space sentinels that will survey the sky in search of space debris.

## 7 REFERENCES

- [1] ATIP-RP-CGS-007, ATIP (Advanced Tracklet Image Processing) Executive Summary, Is 1, 31/07/2014.
- [2] G.F. Gronchi, D. Farnocchia, L. Dimare, Orbit determination with the two-body integrals. II, CMDA 110 (2011) 257–270.
- [3] L. Dimare, D. Farnocchia, G.F. Gronchi, A. Milani, F. Bernardi, A. Rossi, Innovative system of very wide field optical sensors for space surveillance in the LEO region, AMOS conference, Hawaii, 2011, 13 – 16 September.
- [4] A. Milani, and G.F. Gronchi, Theory of orbit determination, Cambridge University Press, 2010.
- [5] Z. Knezevic, A. Milani, Attribution of Survey Observations to Known Solar System Bodies, Publications of the Astronomical Observatory of Belgrade 91 (2012) 185–189.

## Acknowledgements

OHB-I, SpaceDyS and ASI acknowledge funding from the EU H2020 programme under grant agreement 952852 23SST2018-20 H2020-SGA-Space-SST-2019.